Cassini Frequency Selective Subreflector Development

Te-Kao Wu

Jet Propulsion Laboratory, MS:T1 703
California Institute of Technology
4800 Oak Grove Dr.
Pasadena, CA 91109

Abstract

This paper summarizes the design and development of a 4-frequency selective subreflector (FSS) for the NASA Cassini high gain antenna (1 IGA). Specifically, two FSS/I IGA design approaches were considered for multiplexing the four frequency bands (S-,X-, Ku-, and Ka-band) of the Cassini Project. In the first approach (with two transmit and two reflect bands), a double screen FSS with double ring patch elements was developed to transmit the S- and Ku-band signals and to reflect the X- and Ka-band signals. However, this FSS presents relatively high insertion loss at the S-band. Therefore, the Second approach (with one transmit and three reflect bands) was developed, using a single screen FSS with double square loop slot elements to transmit the Ka-band and to rc.fled the S-, X-, and Ku-band waves. Significant improvement in the S-band insertion loss is obtained wit h this secon d approach. However, it will require a dual reflector shaping study to optimize the subreflector size for minimizing the spillover and blockage losses.

I. Introduction

A frequency selective subreflector (FSS) is often employed in the reflector antenna system of a communication satellite [1-3] or a deep space exploration vehicle [4-7] for multi-band operations. In the past, two-bane] FSSs were developed for the high gain antenna (HGA) of the Voyager spacecraft [4] and the Tracking and Data Relay Satellite System ('1'1>1{SS) [1]. Currently, NASA's Cassini Project requires the use of multiple radio frequencies at S-, X-, Ku- and Ka-band for science investigations and data communication links. A single 1 HGA with an FSS subreflector, as illustrated in Figure 1, is proposed to allow a Cassegrain configuration at X-band (7.2, and 8.4 GHz) and Ka-band (32 and 34.5 GHz), and a prime focus configuration at S-band (2.3 GHz) and Ku-band (13.8 GHz). In References [5,8], both single and double screen FSSs were designed with double-square-loop patch elements. The performance of these FSSs arc summarized in 'J'able I and]] for the. single and double screen FSS, respectively. It was noted that the 10ss in the S-band is rather high but it could be reduced significantly by another FSS element design. 'J 'herefore, the objective of this study is to develop new 4-frequency FSSs with significantly improved performance in the S-band while maintaining comparable performance in the other three (X/Ku/Ka) bands.

Two FSS/HGA design configurations arc studied and presented in the following sections. In Section 11, the first design (two-transmit/two-reflect band FSS) approach is described by using double screen FSS with double ring patch elements to transmit the S/Ku band waves and 10 reflect the X/Ka band wave.s. In Section III, another approach (one-transmit/ three-reflect band FSS) with a single screen and double-square-loop (DSL) slot element FSS is demonstrated to transmit the Ka-band waves and to reflect the S/X/Ku band

waves. A waveguide simulator test conducted in the S-band for this single screen FSS is also described. The final section includes some concluding remarks and several recommended future tasks for this research project.

11. Two-Transmit/Two-Reflect Band FSS

The first FSS/HGA configuration considered is the t\\'o-t]a])sl~li(/t\\'o-]e.fleet band case as illustrated in Figure 1. A flat pane] FSS with double-ring (DR) elements was designed and fabricated with a Kevlar honeycomb as shown in Figure 2, As was pointed out earlier this is a two-screen FSS approach. The front FSS (also called the Ka-add-on FSS) is a low-pass FSS, i.e. reflecting Ka-band but transmitting S-, X-, and Ku-band signals. The back FSS is a 3-frequency FSS, i.e. reflecting X-band but transmitting S- and Ku-band signals. The analysis for the DR FSS was described in [6,7]. Representative predicted and measured FSS transmission results arc shown here to prove the validity of the analysis software and design approach. Results will be given first for the single screen FSS then for the double screen 1'Ss.

Figure 3 shows the Ka-add-on FSS design with DR patch elements. The DR patch element array is etched on a 0.005 cm thick Kapton sheet with 1 micron thick copper and then bonded 10 the Kevlar honeycomb sandwich, The measured and computed transmission characteristics of this FSS arc also plotted in Figure 3. only representative transmission results al 30° are given here to demonstrate the good agreement between the computed and measured data. Similarly, Figure 4 shows the DR elements design and the comparison between the computed and measured transmission of a 3-frequency FSS with a Kevlar honeycomb. Note that the resonant frequency is very c1osc to the designated 8.4 GHz for

both TE and TM polarizations even when the incident angle is clanged from normal to 45°. only representative measured data at 0° (normal) incidence is given here to demonstrate the agreement between the computed and measured data. This verifies the accuracy of the analysis and the design approach.

Next, these two single screen FSS were both bonded to a 1.905 cm thick Kevlar honeycomb resulting in a double-screen 4-frequency FSS as depicted in Figure 2. Since the two screens have different lattice geometry, the following single-mode cascading approach was employed to get a first order assessment of this double-screen 1"SS's performance. Consider the double-screen FSS as shown in Figure 2. First, onc divides the FSS al the mid-plane of the Kevlar honeycomb. Upwards from this middle plane is considered the first FSS screen section, and below this plane is the second FSS screen section. 1 :ach FSS section can be accurately modelled by the single screen FSS analysis described in [6,7]. Since the dividing plane is electrically far from the FSS grid and the FSS element spacing is less than a half wavelength, one can assume that only the *0*th order mode is significant. Thus one may next cascade the two sections by converting the scattering matrix [s] from each section 10 a transmission matrix [t] and multiplying the rc.suiting [t] matrices, The final [t] matrix product is then converted back to a scattering matrix, which yields the transmission and reflection coefficients for the double screen FSS.

Figure 5 shows the comparison of the computed and measured transmission results for this double screen FSS. The good correlation between the two results verified this efficient cascading approach. The discrepancy at Ku-band may be attributed to the omission of the anisotropic property of the Kevlar honeycomb in the theoretical model. The insertion losses of this double-screen FSS at all the Cassini frequencies is summarized in Table 3. As

As compared to Tables 1 and 11, little improvement is obtained at S-band. Therefore, the second approach, to be described in next section, was investigated.

111. One-Transmit/Three-Reflect Band FSS

Figure 6 illustrates the configuration of a HGA with the ol~c-tlal~sl~~i t/tlllce-reflect band FSS. in this case, the FSS passes the Ka-band waves while reflecting the S-, X-, and Ku-band waves. This FSS, as depicted in Figure 7, consists of a single screen DSL slot element array etched on a 0.005 cm thick Kapton substrate and then bonded onto a Kevlar honeycomb. The analysis of this FSS is as same as that described in [5]. The computed transmission performance of this single screen FSS is plot ted in Figure 8 as functions of the incident angles and polariz.aliens. As can be seen, the pass-band of this FSS is centered at 33 GHz independent of the variation of incident angles and polarizations. The insertion losses of this FSS are summarized in "J'able 4 for all the Cassini frequencies. The loss at Ka-band is the transmission loss, while the losses at S-, X-, and Ku-band arc reflection losses. Note that the insertion loss at S-band is significantly reduced to less than 0.01 dB.

Representative measured and computed results at 30° incidence arc shown in Figure 9. 'J he good correlation between the two results validates the design approach. It should be pointed out that the measured results at S-band were obtained using the same waveguide simulator technique as described in [9]. Figure 1 O illustrates the FSS waveguide test sample fabricated fox this measurement. Note only the TE polarization case can be measured with this dominant-mode waveguide simulator. 'J he measured transmission and reflection losses at 2.3 G] Iz arc 29.4 dB and 0.29 dB, respectively. The computed results are 31 dB and 0.01 dB, respectively. The correlation between the measured and computed results is fairly good

despite the slight discrepancy which may be attributed to the fabrication tolerance and measurement accuracy limitations.

IV. Conclusion and Recommendations

Two FSS/HGA design configurations, i.e. the two-transmit/two-reflect and the one-transmit/tllrcc-reflect band approaches were successfully demonstrated. Good correlation between the measured and computed results was obtained. This prows the validity of the FSS design and approaches The S-band 10ss is significantly improved by the second approach. Because the S-band feed is put in the Cassegrain feed location for the second approach, the subreflector size is relatively larger to reduce the spillover loss. 1 lowever, one might consider in future research projects reshaping the dual reflector contour to reduce the spillover loss and to keep the subreflector size small. Neverthcless, both approaches give acceptable performance for the Cassini Project.

It is also not cd that some discrepancy exists between the measured and compu t ccl results with the presence of the Kevlar honeycomb. This may be attributed to the present FSS software not taking into account the anisotropy effect of the Kevlar honeycomb. '1 hus one might consider including this anisotropy effect in the model for futu re research projects.

Acknowledgement

The research described in this paper was carried out at the Jet Propulsion 1 aboratory, California institute of Technology, under contract with the National Aeronautics and Space Administration. The author wishes to thank Dr. K. Woo and Dr. W Rafferty for managerial support, Mr. C. Chavez for performing all the measurements, and Mr. G. Hickey for fabricating the Kevlar honeycomb.

References

1. V.D. Agrawal and W.A. Imbriale, "Design of a dichroic Cassegrain subreflector," 11 EEE Trans., vol. AP-27, no.4, pp. 466-473, July 1979.

2. K. Ueno, T. Itanmi, H. Kumazawa, and I. Ohtomo, "Characteristics of FSS for a multi-band communication satellite", 1991 11{10 Int. AP-S Symposium Digest, pp. 735-738, Ontario, Canada, June 1991.

3. S.W. Lee and M, Zimmerman, G. Fujikawa, and R. Sharp, "Designs for the ATDRSS Tri-band reflector antenna," 1991 IEEE Int. AP-S Symposium Digest, pp. 666-669, Ontario, Canada, June 1991.

4. G.] I. Schennum, "Frequency-selective surfaces for multiple frequency antennas," Microwave Journal, vol. 16, pp.55-57, May 1973.

5. T.K. Wu, "Double-square-loop FSS for multiplexing four (S/X/Ku/Ka) bands", 199111 EEE Int. AP-S Symposium Digest, pp. 1885-1888, Ontario, Canada, June. 1991.

6. J. Huang, T.K. Wu and S.W. Lee, "Tri-band FSS with circular ring elements," IEEE Trans. vol. AP-42, no. 2, Feb. 1994.

7. '1'.1{. Wu, S.W. Lee and K. Woo, "Multi-ring element FSS for multi-band applications," 1992 IEEE Int. AP-S Symposium Digest, pp. 1775-1778, Chicago, 11., July 1992.

8. T.K. Wu, "Dielectric measurement of substrate and support materials," Microwave and Optical Technology Letters, vol. 3, no. 8, pp. 283-286, August 1990.

'J'able 1. Computed 1.OSS (dB) of the Single Screen, 4-Frequency, DS I. FSS

Frequency GHz	Θ_i = 0°	30°		45°	
		TE	TM	TE	TM
2 3	.95	1.2	.73	1.6	.5
7.2	.45	.37	.61	.27	.9
8.4	.08	.07	.11	.06	.16
13.8	.37	.56	.29	.9	.2
32	.09	.17	.13	.16	.69
34	.14	.2	.21	.13	.43

Table 2. Comp ed 1.0ss (dB) of the I ouble Scre n, 4-1%1]' ency, DSI FSS

Frequency GHz	Θ_i = 0°	30°		45°	
		TE	TM	TE	TM
2.3	.41	.5	.33	.68	.23
7.2	.65	.73	1.1	.85	1.95
8.4	.14	.17	.19	.22	.29
13.8	1.1	1.2	.73	2.1	.53
32	.53	.19	.22	.21	.48
34	.21	.28	.33	.2	.3

TABLE 3. Insertion Loss (dB) Summary of the Two-Transmit/Two-Reflect Band FSS

Frequency (GHz)	$(\Theta_i, \phi_i) = (0°, 0°)$	(30°, o“)		(45°, 0°)	
		TE	TM	TE	TM
2.3	0.71	0.71	0.5	0.8	0 . 3
7.2	0.43	0.33	0.42	0.37	0,s8
8.4	0.13	0.11	0.15	0.11	0.18
13.8	0.54	0.82	0.57	0.94	0.39
32	0,69	0.(L?	0.71	0.5?,	0.76
34.5	1.09	1.24	1.82	1.29	2.1

Table 4. Computer oss (dB) Summary of he One-T nsmit/Three-Reflec , and IT-S”

Frequency (GHz)	$(\Theta_i, \phi_i) = (0°, 0°)$	(30°, 0°)		(45°, 0“)	
		TE	TM	TE	TM
2.0	0.003	0.002	0.004	0.002	0.006
7.0	0.043	0.033	0.042	0.02	0.07
8.0	0.06	0.04	0.07	0.03	0.09
13.8	0.22	*0.1”/*	0.26	0 . 1 1	0.33
32	0.37	0.42	0.35	0.51	0.32
34.5	0.92	1.34	1.04	2.13	1.03

FIGURE 1. Two Transmit/two reflect band FSS/HGA configuration.

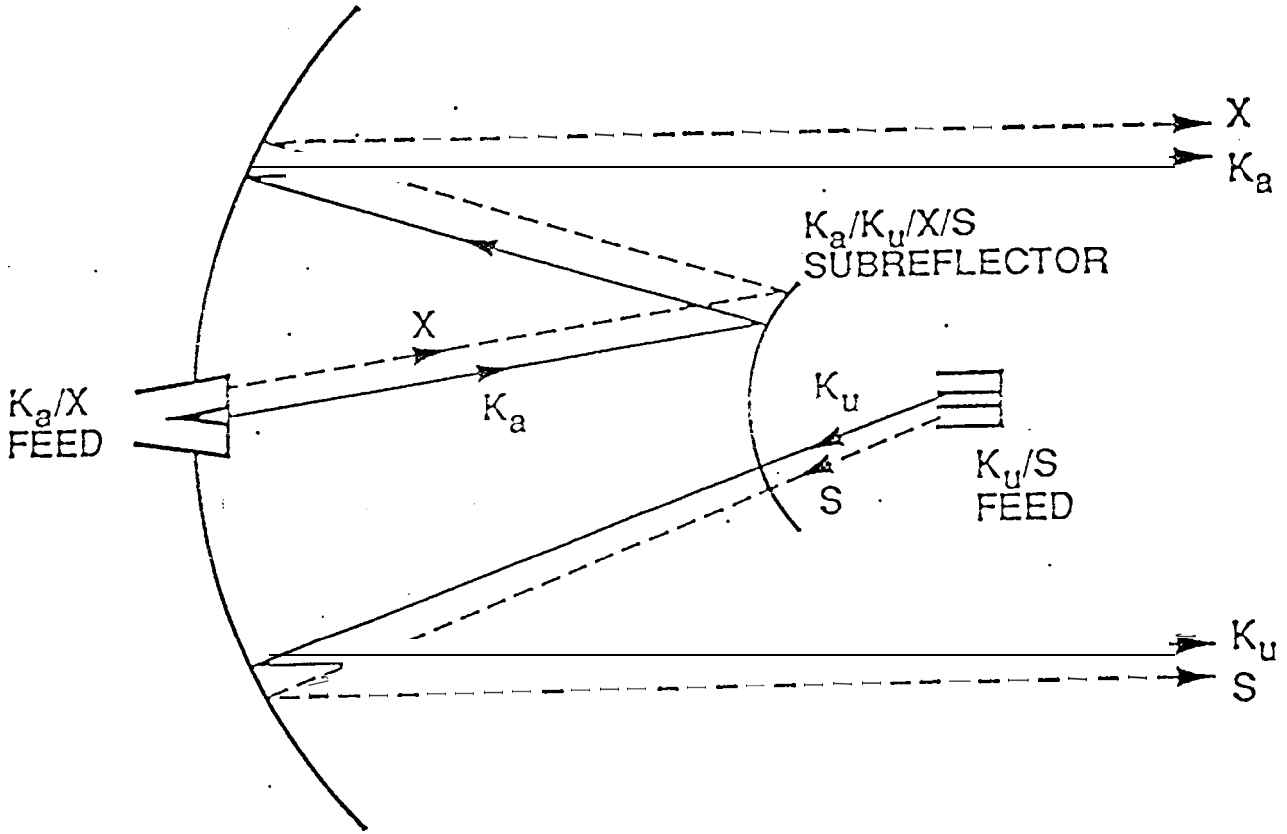

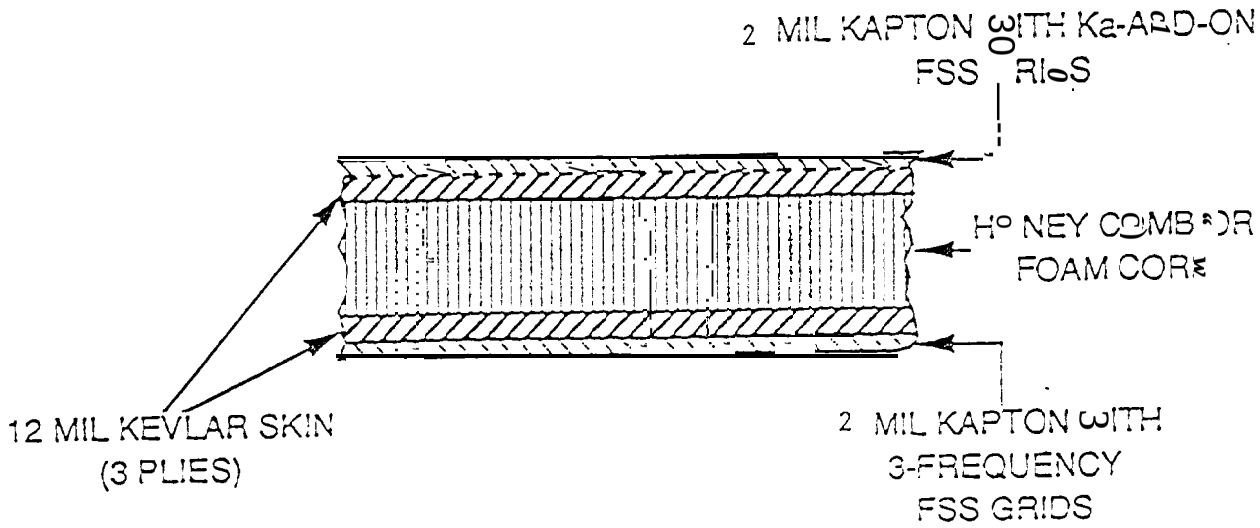

6 FREQUENCY WITH Ka-BAND ADD-ON DESIGN

Figure 2. Two transmit/two reflect band FSS configuration.

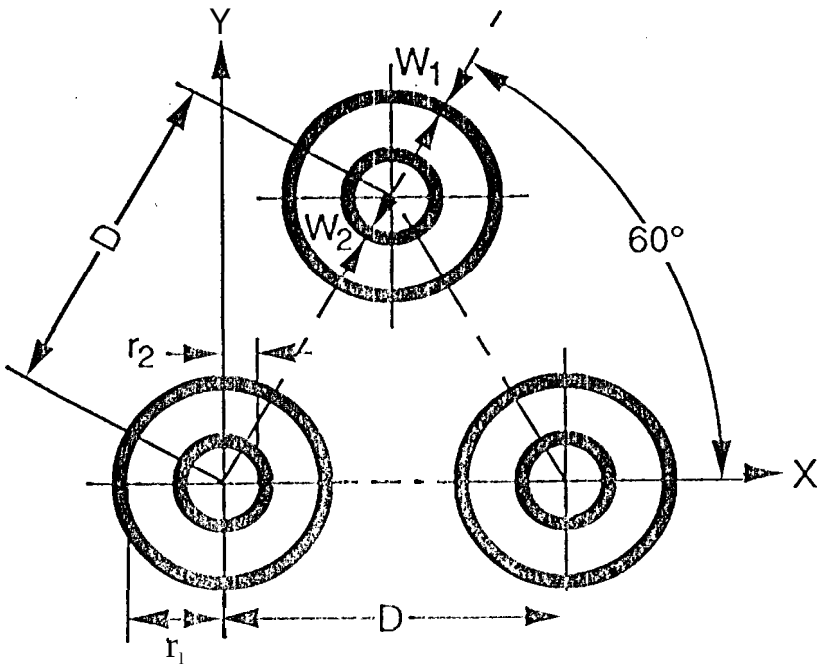

D = .169"
r 1= .047"
r 2 = .028"
w1= w2 = .01"

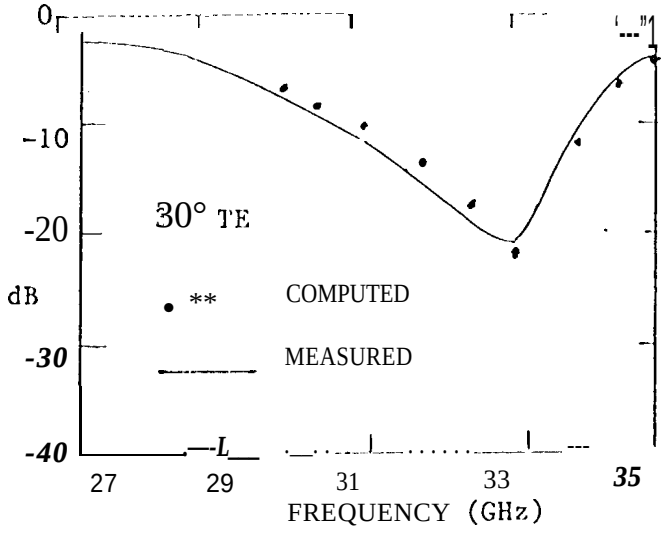

Figure 3. Design and transmission performance of the Ka-add-on FSS with double-ring element.

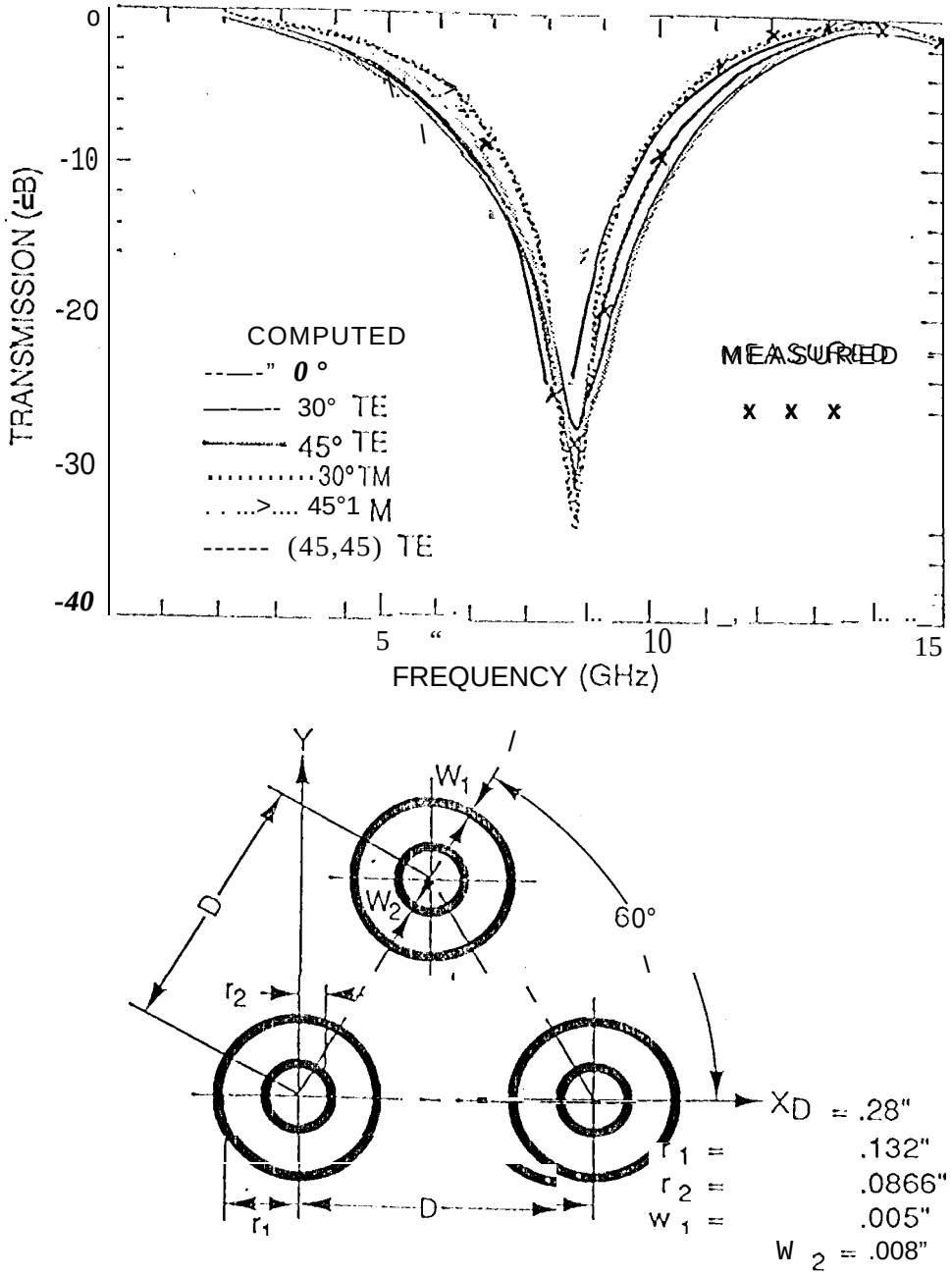

Figure 4. Design and transmission performance of the three-frequency FSS with double-ring element.

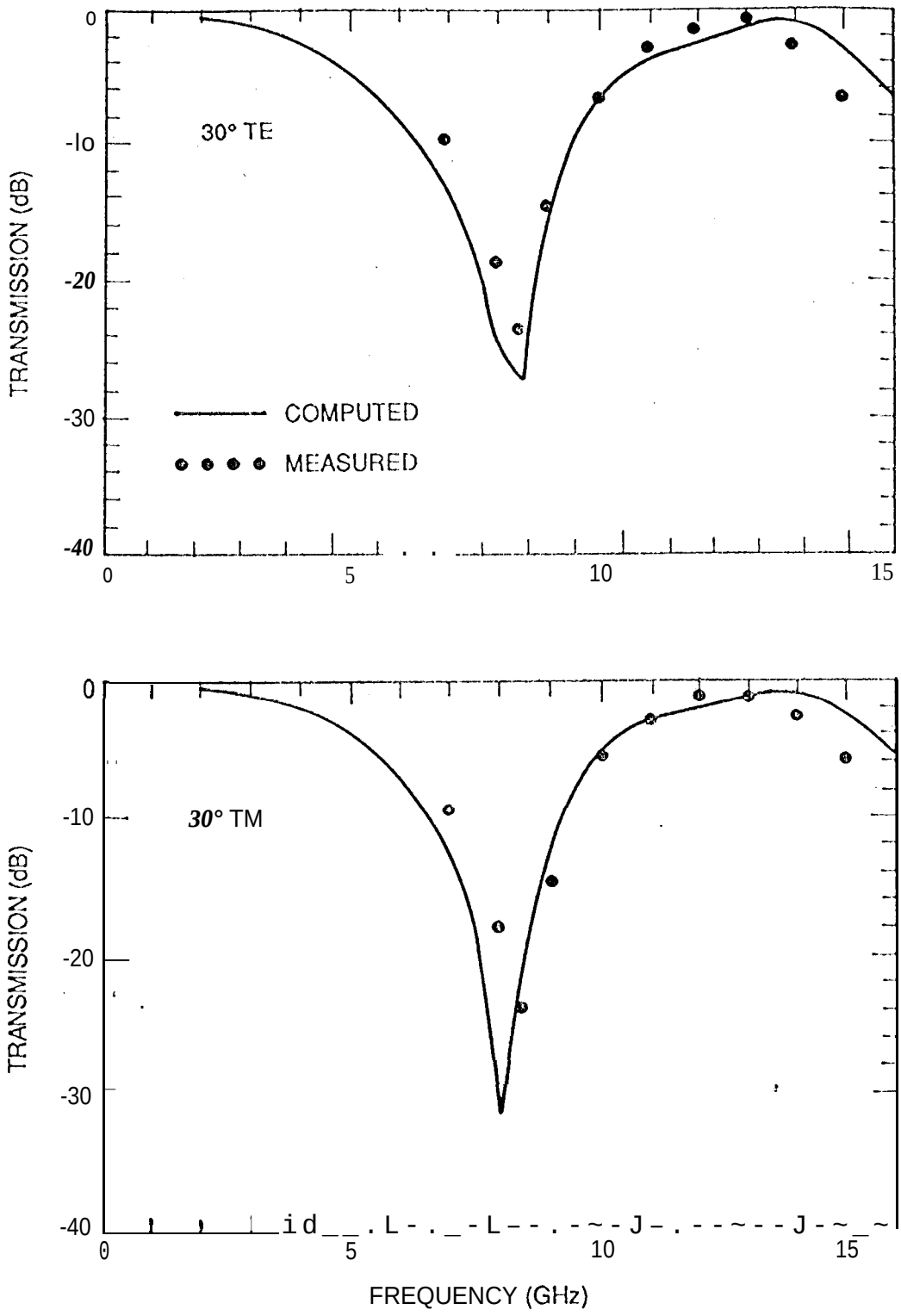

Figure 5. Comparison of measured and computed transmission characteristics of the Two transmit/two reflect band FSS.

FIGURE 6. One transmit/three reflect band FSS/HGA configuration.

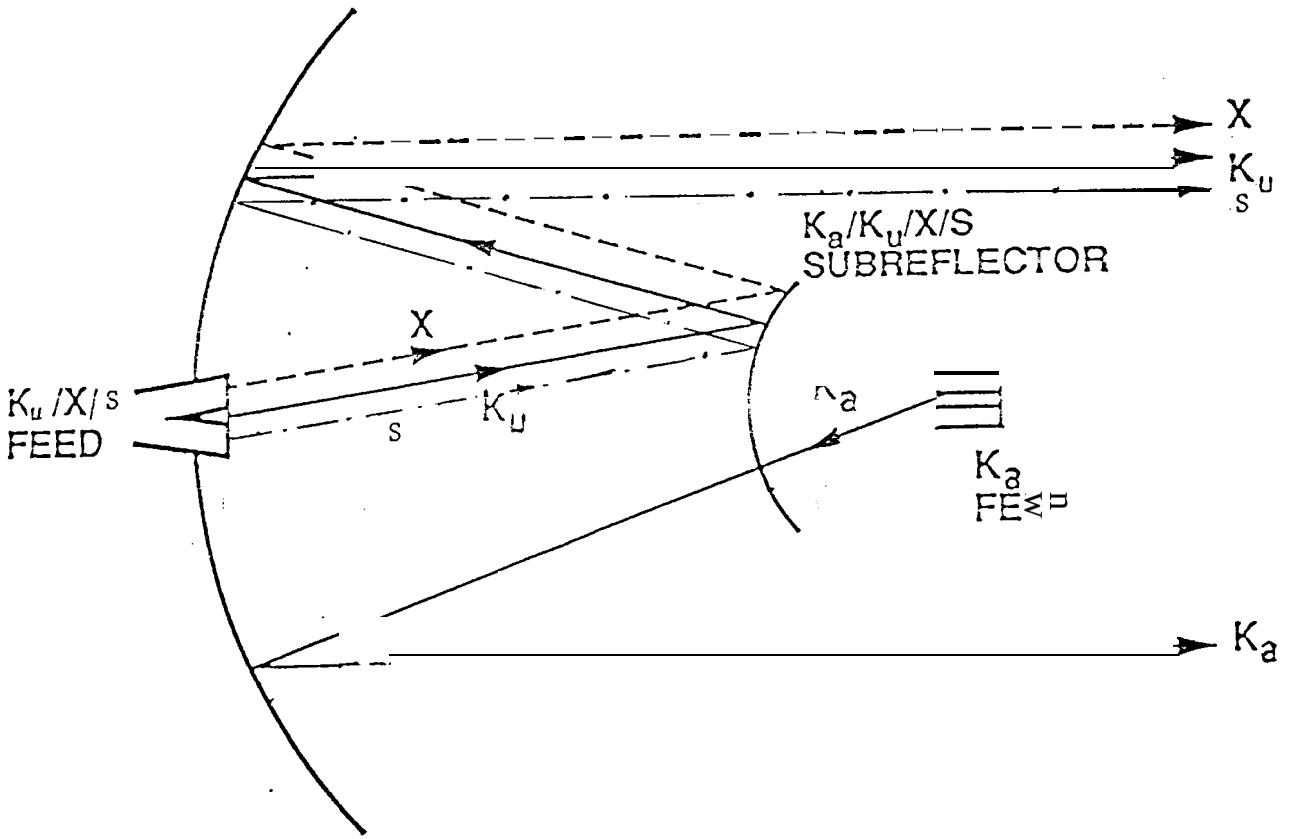

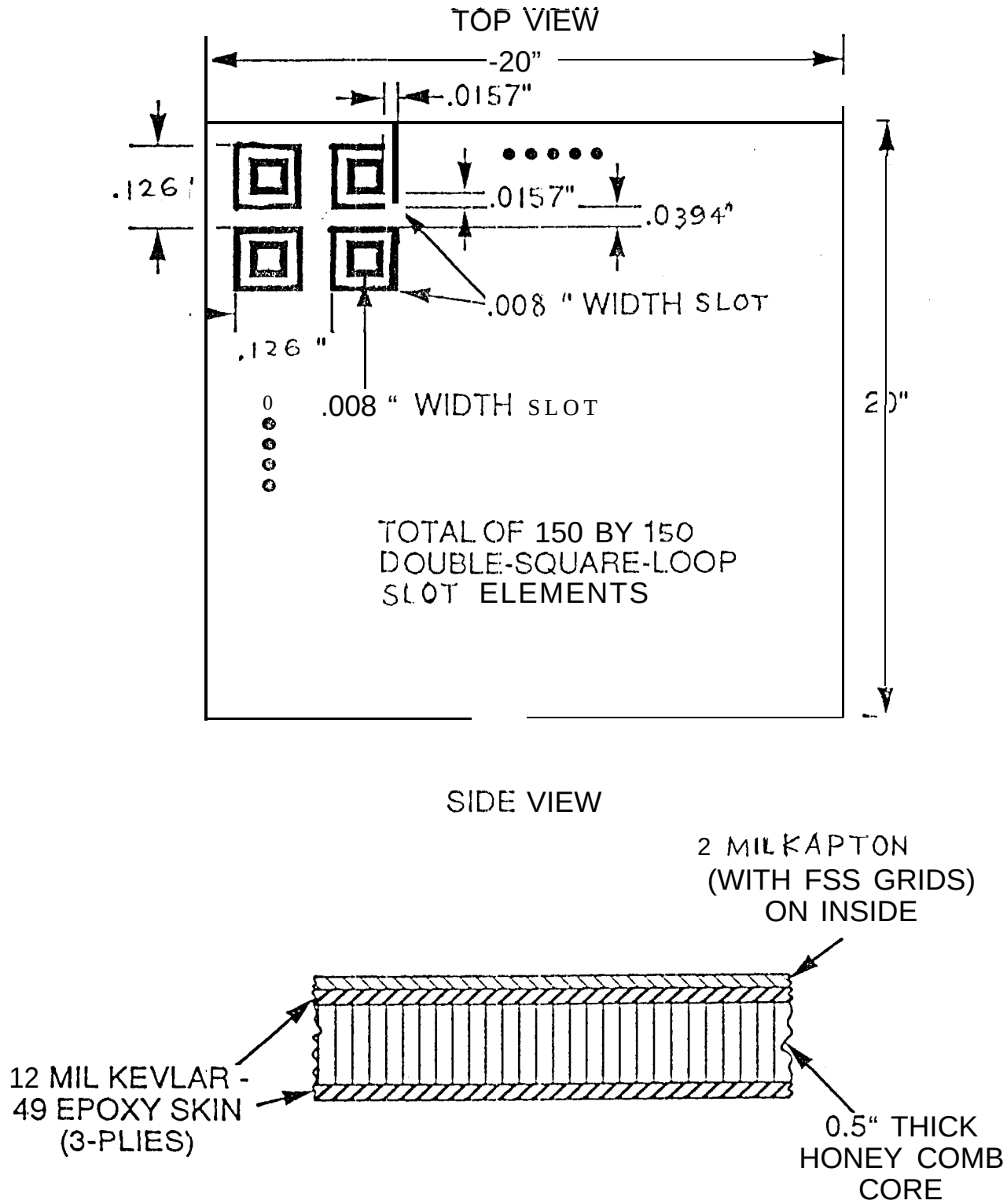

Figure 7. Configuration of the double-square-loop element, 4-frequency integrated FSS with a Kevlar honeycomb.

Figure 8. Computed transmission performance of the One transmit/three reflect band FSS.

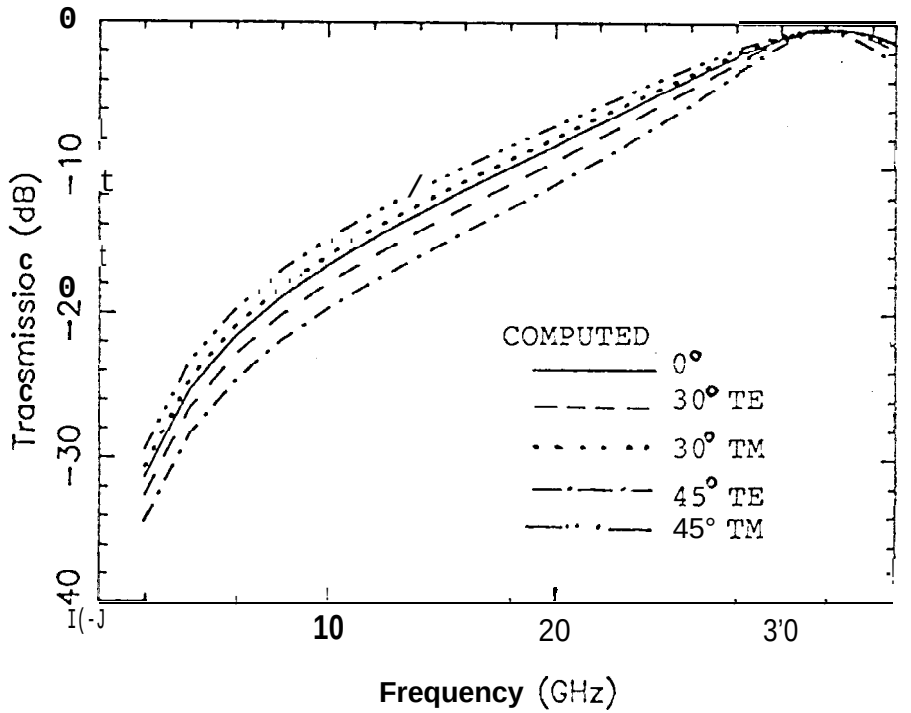

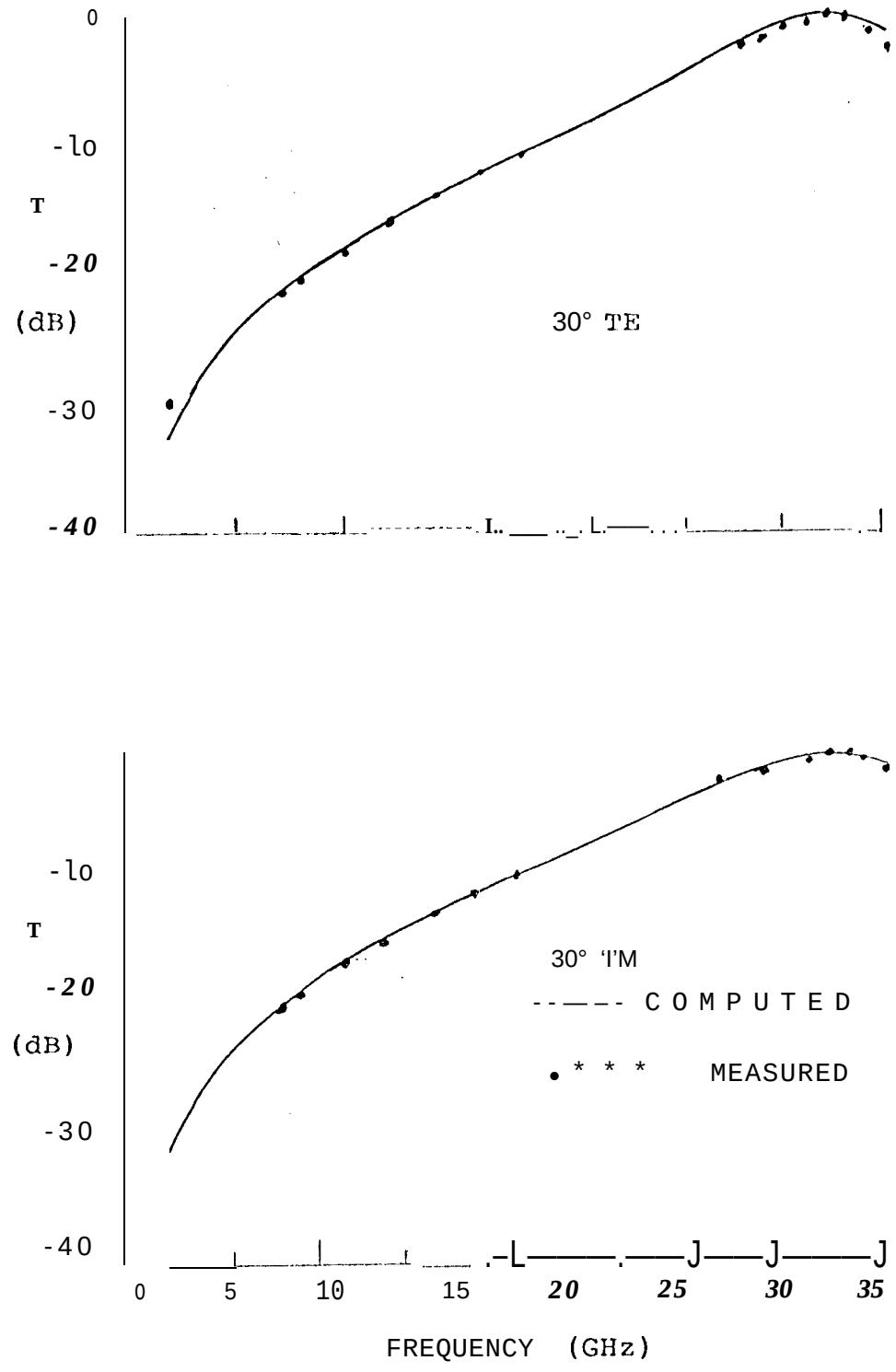

Figure 9. Comparison of measured and computed transmission characteristics of the One transmit/three reflect band FSS.

Figure 10. Photo of the test sample for the waveguide simulator test.